Ambient-Stable, Annealing-Free, and Ambipolar Organic Field-Effect Transistors Based on Solution-Processable Poly(2,2′-bis(trifluoromethyl)biphenyl-*alt*-2,5-divinylthiophene) without Long Alkyl Side Chains

Chi-Jui Chiang, Jyh-Chien Chen, Hsiang-Yen Tsao, Kuan-Yi Wu, and Chien-Lung Wang**

An ambipolar conjugated polymer CF$_3$-PBTV, poly(2,2′-bis(trifluoromethyl) biphenyl-*alt*-2,5-divinylthiophene), consisting of thienylenevinylene as the donor and trifluoromethyl-substituted biphenyl as the acceptor has been successfully synthesized. CF$_3$-PBTV shows solution-processability without electrically insulating long alkyl side chains. Grazing incidence X-ray diffraction results suggest a nearly equal population of flat-on and end-on domains in CF$_3$-PBTV thin film. The excellent ambipolarity of CF$_3$-PBTV is demonstrated by well-equivalent charge mobilities of 0.065 and 0.078 cm^2 V^{-1} s^{-1} for p- and n-channel, respectively. The organic field-effect transistors (OFET) also shows very high on/off ratio (≈10^7) which is attributed to the relatively large bandgap and low-lying highest occupied molecular orbital (HOMO) of CF$_3$-PBTV. The OFET performance barely changes after the device is stored in ambient conditions for 90 days. The ambient-stability is attributed to the enhanced oxidative stability from its low-lying HOMO and the better moisture resistance from its fluorine contents. The performance of CF$_3$-PBTV based OFET is annealing independent. It is noteworthy that the solution-processable, ambipolar, and thienylenevinylene-containing conjugated polymer without any long alkyl side chains is reported for the first time. And to the best of our knowledge, it is the first ambient-stable, annealing-free OFET with well-equivalent ambipolarity.

1. Introduction

Organic field-effect transistors (OFETs) have drawn intensive attention due to their potential applications in ink-jet printed flexible sensors, logic circuits, radiofrequency identification tags, and displays.[1] Therefore, significant efforts have been made toward the development of high performance conjugated semiconducting polymers used as the active layer in OFETs due to their solution-processability and mechanical robustness.[2] Conjugated semiconducting polymers are commonly classified as either n-type or p-type materials, which typically show unipolar property in their OFET performance.[3] P-type conjugated polymers with high hole mobility have been developed over a decade since most of conjugated polymers are known to be π-electron excessive in nature.[4] On the contrary, promising n-type conjugated polymers were only obtained after strong electron-withdrawing moieties such as diketopyrrolopyrroles (DPP),[5] benzobisthiadiazole,[6] benzo[*c*]cinnolines,[7] isoindigos,[8] benzodipyrrolidones,[9] naphthalene diimides,[10] cyano groups,[11] and halogens[12] were incorporated into the backbone architecture. These electron-withdrawing moieties enhance the electron affinity, deepen the lowest unoccupied molecular orbital (LUMO) energy levels, and thus facilitate the electron transport and injection. P- and n-type conducting channels in transistors based on Si-technology are well-known to be readily accessible by implantations of dopants. However, laterally controlled deposition of two different organic materials on a substrate could lead to processing complexity. Therefore, conjugated polymers, which contain both n- and p-type characteristics and thus realize the ambipolar OFET without complex patterning techniques are desirable. Recently, through proper side chain and main chain engineering, ambipolar DPP-based copolymers with both remarkably high hole and electron mobilities over 1 cm^2 V^{-1} s^{-1} have been reported.[13]

Among the reported electron-withdrawing moieties, fluorine atom has attracted special attention due to its unique properties, such as small van der Waals radius of 1.35 Å and the highest Pauling electronegativity of 4.0. It has been reported that the fluorination of conjugated polymers alters their OFET characteristics from p-type, ambipolar, to n-type.[14] In virtue of the strong electronegativity of fluorine atoms, the fluorination of conjugated polymers lowers not only the LUMO but also highest occupied molecular orbital (HOMO), which facilitates electron injection from source/drain electrode[15] and enhances the oxidative stability,[16] respectively. Moreover, due to the hydrophobicity of fluorine atoms, the resistance to the diffusion

C.-J. Chiang, Prof. J.-C. Chen, H.-Y. Tsao
Department of Materials Science and Engineering
National Taiwan University of Science and Technology
43, Sec. 4 Keelung Road, Taipei 10607, Taiwan
E-mail: jcchen@mail.ntust.edu.tw
K.-Y. Wu, Prof. C.-L. Wang
Department of Applied Chemistry
National Chiao Tung University
1001 Ta Hsueh Road, Hsin-Chu 30010, Taiwan
E-mail: kclwang@nctu.edu.tw

DOI: 10.1002/adfm.201403428

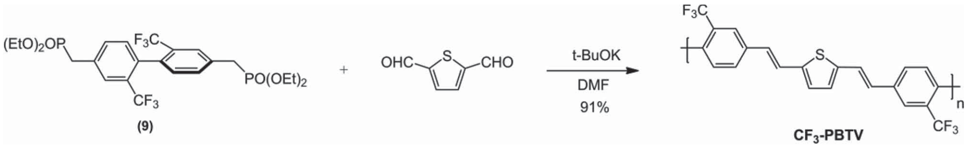

Scheme 1. Synthesis of CF_3-PBTV by Horner–Emmons polymerization.

of moisture is improved, which could prevent the susceptible organic radical anions that could form n-channel from deactivation by moisture. Combined with the enhanced thermal stability resulted from high dissociation energy of C–F bonds, the lifetime of OFETs based on fluorinated conjugated polymers in ambient conditions could be improved.[17] Furthermore, the introduction of fluorine atoms into polymer backbone has been reported to lead to fluorophobic and fluorophilic effects.[18] The unique interaction between C–F and C–H in fluorinated polymers may promote F-induced molecular orientation and crystallization,[19] which may have dramatic effects on the carrier transport in OFETs.

The processability of conjugated polymers depends strongly on their solubilizing side chains.[20] Long side chains, such as ethylhexyloxy,[21] hexyldecyl,[22] dimethyloctyloxy,[23] and siloxane-terminated alkyl[13c,d,24], are essential to provide sufficient solubility to the conjugated polymers. These solubilizing side chains also play important roles in charge mobilities by changing the π-stacking distance of conjugated polymers. However, the solubilizing side chains are known to be electrically insulating and are detrimental to the charge injection and transport.[25] For example, the hole mobility of sexithiophene was found to decrease dramatically from 1.1 to 0.1 $cm^2 V^{-1} s^{-1}$ when the ethyl side chains were replaced by the longer decyl groups.[26] Moreover, the electron mobility was found to be one order of magnitude lower in melt-annealed edge-on P(NDI2OD-T2) (0.021 $cm^2 V^{-1} s^{-1}$) than that of commonly spin-coated face-on P(NDI2OD-T2) (0.1–0.2 $cm^2 V^{-1} s^{-1}$) film.[3a,27] The result implies that the long alkyl side chains attached on edge-on polymers tend to form intrinsic insulating barriers separating the active layer from the electrodes and dielectric layer, which impedes charge injection and transport. Therefore, the tradeoff between processability and charge mobility remains an obstacle for designing highly efficient solution-processable conjugated polymers.

Fluorine-substitution has been successfully used in fine-tuning the energy levels and OFET characteristics of conjugated oligomers[28] and polymers.[29] However, without solubilizing alkyl side chains, solution-processable fluorinated conjugated polymers have not yet been reported. In this study, we report the design and synthesis of a novel thienylenevinylene-based conjugated polymer, poly(2,2′-bis(trifluoromethyl) biphenyl-*alt*-2,5-divinylthiophene), abbreviated CF_3-PBTV, with 2,2′-bis(trifluoromethyl)biphenyl (CF_3-BP) unit as the acceptor. Our study demonstrates for the first time a solution-processable ambipolar conjugated polymer without long alkyl side chains for OFET application. CF_3-PBTV delivers well-equivalent ambipolarity with hole mobility of 0.062 $cm^2 V^{-1} s^{-1}$ and electron mobility of 0.071 $cm^2 V^{-1} s^{-1}$ without the needs of thermal post-treatments. Furthermore, this ambipolar OFET with very high on/off ratio (≈10^7) shows excellent stability in ambient conditions for 90 days. To the best of our knowledge, it is the first ambient-stable and annealing-free ambipolar OFETs with well-equivalent ambipolarity.

2. Results and Discussion

CF_3-PBTV was synthesized by polymerization between 2,2′-bis(trifluoromethyl)-4,4′-bis(diethyl methylenephosphonate)biphenyl (9) and thiophene-2,5-dicarbaldehyde in N,N-dimethylformamide (DMF) in the presence of potassium *tert*-butoxide (*t*-BuOK) as the base, as shown in **Scheme 1**. The diphosphonated monomer (9) was synthesized through an eight-step synthetic route, as shown in Scheme S1, Supporting Information. The chemical structures of monomer (9) and novel CF_3-PBTV were well characterized as shown in the Experimental Section and in Figures S1, S2, S3, and S4, Supporting Information. Since the biphenyl unit is not coplanar due to the steric hindrance between the trifluoromethyl substituents, the coplanar 2,5-bis((E)-3-(trifluoromethyl)styryl)thiophene conjugated segment is illustrated as the repeating unit of CF_3-PBTV as shown in Scheme 1. The repeating unit can be considered as thiophene at the center, linked by vinylenes then trifluoromethyl-substituted phenyls. Vinylene linkages are easily accessible by the well-known Gilch reaction between bis-halomethyl compounds. However, the inevitable formation of *cis-trans* isomers and structural defects during Gilch polymerization have been reported to be detrimental to the performance in electronic devices.[30] Therefore, Horner–Emmons polymerization[31] which was reported to form all-trans and defect-free vinylene linkages was adopted in our research. CF_3-PBTV had a number-average molecular weight (M_n) of 13 000 g mol^{-1} and a polydispersity index (M_w/M_n) of 1.92, measured by gel permeation chromatography (GPC) in dimethylacetamide (DMAc) using polystyrene standards, as shown in **Table 1** and Figure S5, Supporting Information. CF_3-PBTV also exhibited excellent thermal stability with a glass transition temperature of 190 °C (Figure S6, Supporting Information) and a decomposition temperature of 436 °C (5% weight loss in N_2 atmosphere, as shown in Figure S7, Supporting Information), which is around 80–100 °C higher than those of alkylated thienylenevinylene-containing

Table 1. Molecular weight and thermal properties of CF_3-PBTV.

$M^{a)}$ [g mol^{-1}]	$M_w$$^{a)}$ [g mol^{-1}]	PDI$^{a)}$	Yield [%]	$T_g$$^{b)}$ [°C]	$T^{c)}$ [°C]	Char yield$^{d)}$ [wt%]
13 000	25 000	1.92	90.7	190	436	56

a)Obtained from GPC using DMAc as solvent and calibrated with polystyrene standards; b)Measured by DSC at a heating rate of 10 °C min^{-1} in nitrogen; c)Measured by TGA at a heating rate of 10 °C min^{-1} in nitrogen; d)Residual weight percentage at 800 °C in nitrogen.

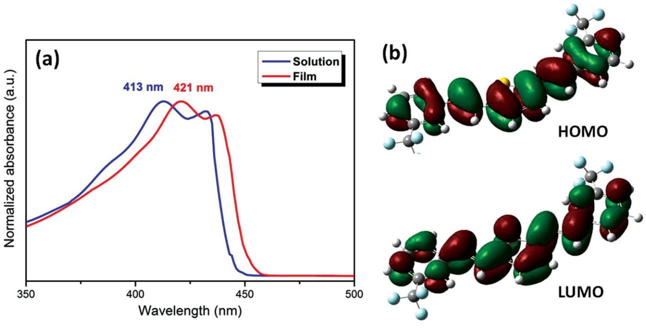

Figure 1. a) UV–vis spectra and b) DFT-simulated distribution contours of CF$_3$-PBTV.

counterparts.[32] The enhancement in thermal stability can be attributed to the stronger C–F bonds of trifluoromethyl groups.

CF$_3$-PBTV was soluble in common organic solvents such as DMF, N-methylpyrrolidone (NMP), dichloromethane (DCM), chloroform, toluene, and dichlorobenzene (DCB). Without long alkyl side chains, CF$_3$-PBTV exhibits excellent solution-processability because of the twisted CF$_3$-BP structural unit, which has been proved to effectively increase the solubility of various rigid polymers.[33] In particular, it is noteworthy that this is the first organosoluble thienylenevinylene-containing conjugated polymers without any long alkyl/alkoxy solubilizing side chains.

UV–vis absorption spectra of a dilute CF$_3$-PBTV solution in tetrahydrofuran (THF) (10^{-5} M) and a spin-coated thin film on quartz substrate are shown in **Figure 1**a. In the case of CF$_3$-PBTV dilute solution, a maximum absorption at wavelength $\lambda_{\max} = 413$ nm and a vibronic absorption shoulder at wavelength $\lambda_s = 432$ nm were observed, while the absorption peaks in spin-coated thin films were slightly red-shifted to 421 and 437 nm, respectively. The well-defined vibronic features imply the existence of some structural organization of molecules. An analogue conjugated polymer without thiophene moieties, PBPV, poly(2,2'-bis(trifluoromethyl)-*p*-biphenylene vinylene), (M_n: 15 000 g mol^{-1}), was also prepared for the comparison as described in the Experimental Section and characterized in Figures S8 and S9, Supporting Information. The maximum absorption peak of CF$_3$-PBTV was red-shifted relative to that of PBPV (321 nm, **Table 2**), indicating the extension of effective conjugation length by the introduction of 2,5-divinylthiophene between two trifluoromethyl-substituted phenyls.

The electrochemical redox properties of CF$_3$-PBTV thin films were measured by cyclic voltammetry (CV). The oxidation and reduction onset potentials of CF$_3$-PBTV were 0.59 and –1.44 eV, respectively, as shown in Figure S10, Supporting Information. The HOMO (ionization potential, IP) and LUMO (electron affinity, EA) energy levels were calculated from the onset potentials of oxidation and reduction. The absolute energy level of ferrocene/ferrocenium (Fc/Fc$^+$) was assumed to be 4.8 eV below vacuum level. The external Fc/Fc$^+$ redox standard $E_{1/2}$ was estimated to be 0.09 V versus Ag/Ag$^+$ in acetonitrile with our CV system. The calculated HOMO and LUMO energy levels of CF$_3$-PBTV were –5.30 and –3.27 eV, respectively. The electrochemical bandgap calculated from CV measurement was 2.03 eV. The narrower bandgap of CF$_3$-PBTV (2.03 eV) compared to that of PBPV (2.90 eV, Table 2) indicates the extension of effective conjugation length by introducing 2,5-divinylthiophene between two trifluoromethyl-substituted phenyls.

In addition, the HOMO energy level of CF$_3$-PBTV (–5.30 eV) was 0.64 eV higher than that of PBPV (–5.94 eV, Table 2) when measured under the same conditions. This result is in good agreement with the electron-donating effect of thiophene moieties. However, the HOMO energy level of CF$_3$-PBTV is around 0.3 eV deeper than those of low-bandgap thienylenevinylene-containing counterparts.[32] The low-lying HOMO energy level (–5.30 eV) resulted from the introduction of strong electron-withdrawing trifluoromethyl groups could be beneficial to the air stability.[34] Therefore, CF$_3$-PBTV based OFETs are expected to be more stable compared to those based on low-bandgap thienylenevinylene-containing counterparts under ambient conditions.

To access the molecular geometry and frontier orbital distributions of CF$_3$-PBTV, the theoretical calculation was conducted on the repeating unit of CF$_3$-PBTV with density functional

Table 2. Optical and electrochemical properties of CF$_3$-PBTV and PBPV. *s*: Adsorption shoulder.

Polymer	Solution $\lambda_{abs}$$^{a)}$ [nm]	Film $\lambda_{abs}$$^{b)}$ [nm]	HOMO$^{c)}$ [eV]	LUMO$^{d)}$ [eV]	$E_g$$^{e)}$ [eV]
CF$_3$-PBTV 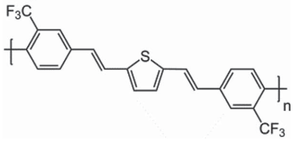	413*s*, 432*s*	421*s*, 437*s*	–5.30	–3.27	2.03
PBPV 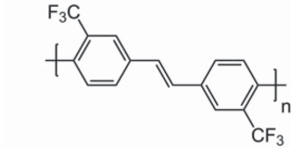	321	345	–5.94	–3.04	2.90

$^{a)}$Measured in THF solution with a concentration of 10^{-5}M; $^{b)}$Measured with polymer spin-coated on quartz substrate; $^{c)}E_{HOMO} = -(E_{onset}{}^{ox} + 4.80 - 0.09)$ (eV) measured by cyclic voltammetry; $^{d)}E_{LUMO} = -(E_{onset}{}^{red} + 4.80 - 0.09)$ (eV) measured by cyclic voltammetry; $^{e)}E_g = \mathrm{IP}(E_{onset}{}^{ox}) - \mathrm{EA}(E_{onset}{}^{red})$ (eV).

theory (DFT) using the B3LYP functional[35] and the 6–31 G** basis set[36] as implemented in GAUSSIAN 09. The energy-minimized geometry of CF_3-PBTV repeating unit was simulated to be coplanar. The dihedral angles between thiophene and vinylene linkage (ψ_1, $\psi_{1'}$) and the dihedral angles between trifluoromethyl-substituted phenyl and vinylene linkage (ψ_2, $\psi_{2'}$) were calculated to be 0° as shown in Figure S11, Supporting Information. The coplanar conformation of the repeating unit is beneficial to the charge transport in this region. The calculated HOMO and LUMO distribution contours of CF_3-PBTV are shown in Figure 1b. Owning to the coplanarity and the unique match of trifluoromethyl-substituted phenyl acceptor and thienylenevinylene donor, the HOMO and LUMO distribution contours are both uniformly distributed in the repeating unit. The uniformly delocalized HOMO and LUMO distribution contours are expected to promote the ambipolarity.

The packing structures of the polymer chains in the thin-film were analyzed by grazing incidence X-ray diffraction (GI-XRD) measurement as shown in **Figure 2**a,b. The samples were prepared following the same procedures for OFET devices without gold electrodes. Two diffraction peaks at 4.79° (*d*-spacing of 18.4 Å) and 9.58° (*d*-spacing of 9.2 Å) can be found both along the q_{xy} (in-plane) and q_z (out-of-plane) directions. Figure 2c shows the energy-minimized molecular model of CF_3-PBTV. Unlike most conjugated polymers, CF_3-PBTV lacks long lateral alkyl chains, and has a small lateral dimension. Thus, the lateral dimension of CF_3-PBTV is not sufficient for a periodic stacking with *d*-spacing of 18.4 Å. On the other hand, the length of a CF_3-PBTV repeating unit matches the 18.4 Å *d*-spacing (Figure 2c). Consequently, it is most likely that the diffractions in the GI-XRD measurement originated from the periodicity along the chain axis. The diffractions along the q_{xy} direction thus suggest the presence of the flat-on CF_3-PBTV domains, and the diffractions along the q_z direction indicate the presence of the end-on CF_3-PBTV domains, as illustrated in Figure 2d. Furthermore, the similar diffraction intensities along the q_{xy} and q_z directions suggest that the populations of the flat-on and end-on CF_3-PBTV domains on the substrate are nearly identical. In general, flat-on orientation is a preferable orientation in the spin-coated films of conjugated polymers. Only few examples of end-on conjugated polymers have ever been reported. Moreover, in most cases, extra processes, such as surface-initiated polymerization from the Si substrate,[37] infiltration of polymers in oriented nanopores,[38] solvent–vapor treatments,[39] nanoprinting,[40] or polymer blending were involved.[41] The end-on orientation of conjugated polymers achieved without complicated processes remains rare.

In our case, the fluorocarbon (trifluoromethyl groups) substitutions on the CF_3-PBTV backbone are well-known for their lipophobicity and low surface energy.[29] The unfavorable interaction between the hydrocarbons of *n*-octadecyltrichlorosilane (OTS) self-assembled monolayer (SAM) on the SiO_2 surface and trifluoromethyl lateral groups of CF_3-PBTV may give the driving force for the end-on orientation.[42] Thus, the result demonstrates the potential of the trifluoromethyl lateral groups in controlling the chain orientation of conjugated polymers in the thin-film state. Since the intramolecular charge transport has been reported to be faster than the intermolecular charge hopping,[43] the end-on conjugated polymers might facilitate effective vertical intramolecular charge transport. Such effects

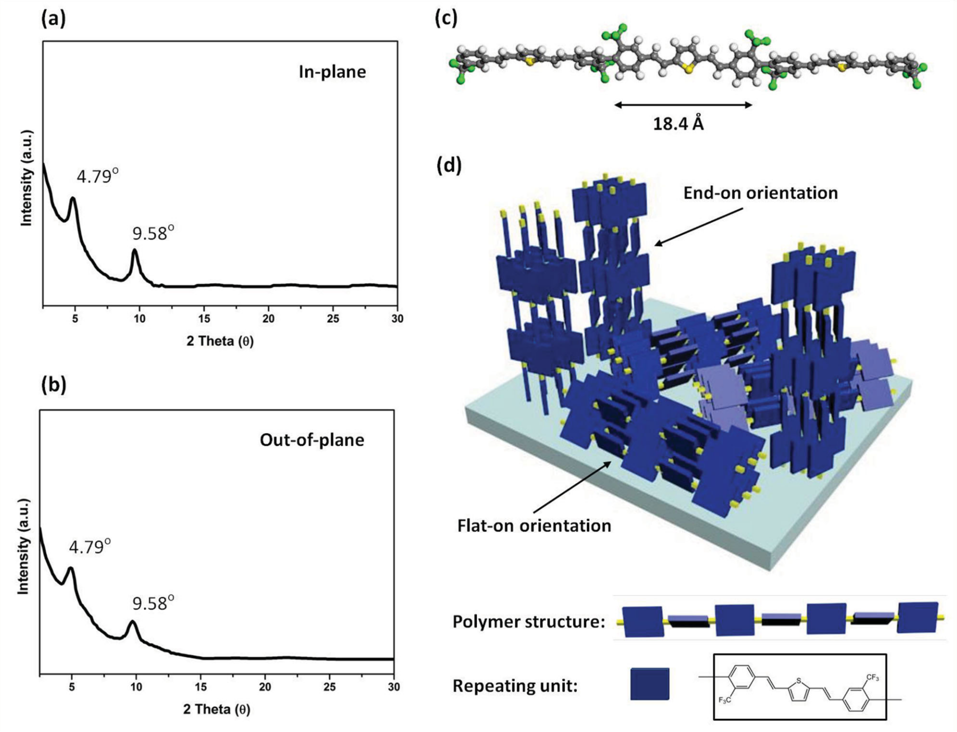

Figure 2. a) In-plane and b) out-of-plane GI-XRD patterns of CF_3-PBTV thin film. c) Energy-minimized molecular model of CF_3-PBTV and d) illustration of the molecular orientations of CF_3-PBTV on the substrate.

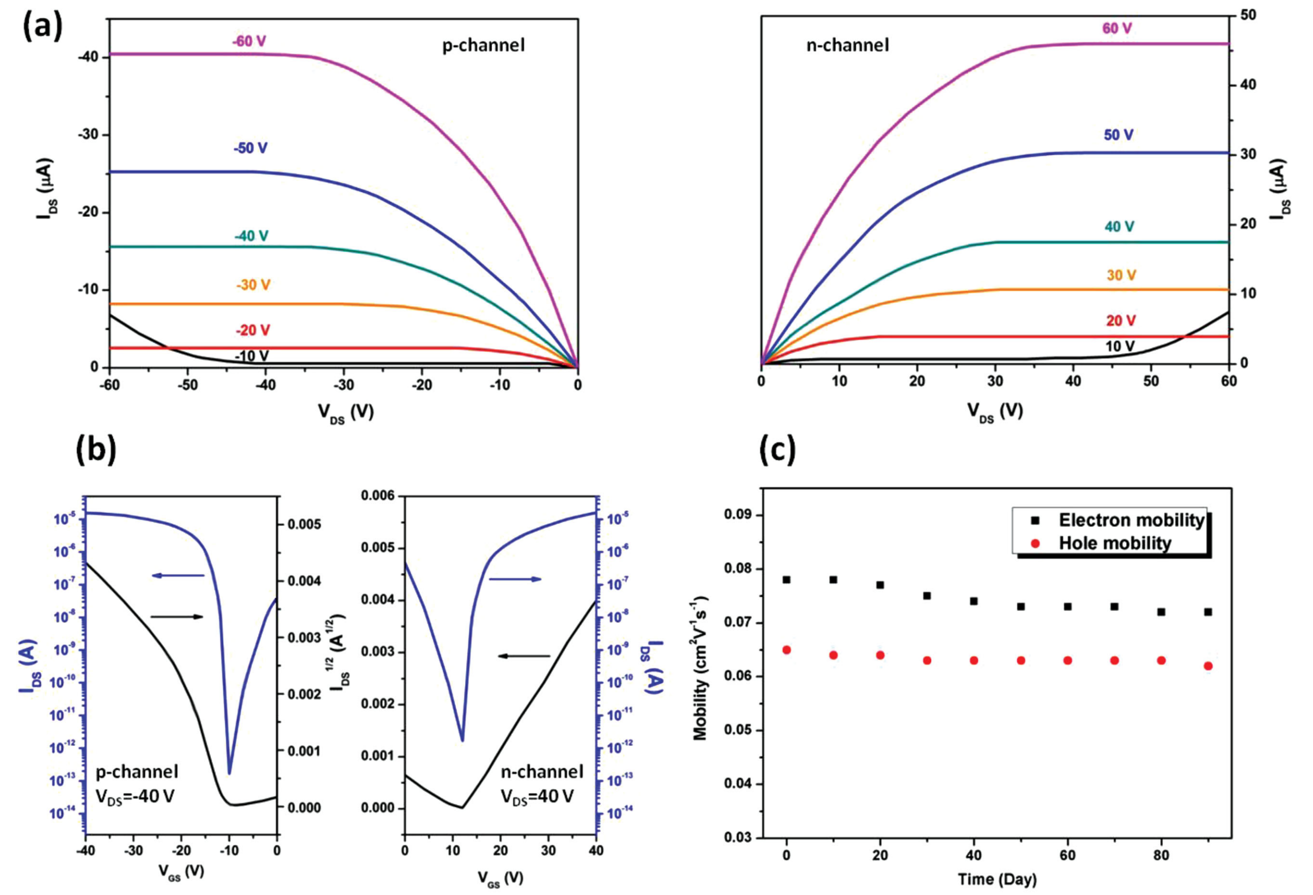

Figure 3. a) Ambipolar output curves, b) ambipolar transfer curves, and c) ambient-stability of CF_3-PBTV based OFET.

in the applications like organic photovoltaic cells, where vertical charge transport is crucial, will be further explored.

The OFET characteristics of CF_3-PBTV were investigated using the bottom-gate/top-contact device configuration with gold (Au) as source and drain electrodes. Heavily *n*-doped silicon (n^+-Si) and SiO_2 were used as the gate electrode and dielectric insulator (capacitance C_i = 11 nF cm^{-2}), respectively. The SiO_2 dielectric insulator was treated with OTS-SAM to passivate the SiO_2 surface and prevent electron-trapping by OH groups. An anhydrous solution of CF_3-PBTV (5 mg mL^{-1}) in DMF was deposited by spin-coating (1000 rpm, 30 s) onto the OTS-modified SiO_2/n^+-Si substrate at room temperature. The drain and source electrodes were deposited by thermal deposition of gold through a shadow mask. The channel width (*W*) and length (*L*) were 2000 and 50 μm, respectively. All OFET fabrication processes and characteristic measurements, except SiO_2 growth and gold deposition, were performed in ambient conditions. The OFET characteristics are summarized in **Figure 3** and **Tables 3** and **4**.

As summarized in Table 3, the CF_3-PBTV based OFET exhibited hole mobility (μ_h) of 0.065 cm^2 V^{-1} s^{-1} and electron mobility (μ_e) of 0.078 cm^2 V^{-1} s^{-1}, extracted from the saturation regime. As mentioned above, the long side chains are generally known to be electrically insulating in nature, and are detrimental to the charge injection and transport. In our case, CF_3-PBTV lacks long lateral electrically insulating side chains which could form insulating barriers for charge transport. Therefore, the charge transport could be more efficient in CF_3-PBTV than in most of the long-alkyl-chain-containing counterparts. The well-equivalent ambipoalrity, as shown in Figure 3, indicates

Table 3. Characteristics and ambient-stability of CF_3-PBTV based OFET.

	As-fabricated			30 days[a]			90 days[a]		
	Mobility[b] $[cm^2\ V^{-1}\ s^{-1}]$	V_{th} [V]	I_{on}/I_{off}	Mobility[b] $[cm^2\ V^{-1}\ s^{-1}]$	V_{th} [V]	I_{on}/I_{off}	Mobility[b] $[cm^2\ V^{-1}\ s^{-1}]$	V_{th} [V]	I_{on}/I_{off}
p-channel	0.065	–11	10^7	0.063	–11	10^7	0.062	–11	10^7
n-channel	0.078	12	10^7	0.075	12	10^7	0.071	12	10^7

[a] Long-term stability of OFET was investigated under ambient conditions; [b] Mobilities were calculated using equation $\mu = 2I_{DS}L\ [C_iW(V_{GS} - V_{th})^2]^{-1}$. ($\mu$ = mobility, L = length, C_i = Capacitance, W = width, V_{th} = threshold voltage).

Table 4. OFET characteristics based on CF_3-PBTV with various annealing temperature.

	Annealed at 120 °C[a)]			Annealed at 180 °C[a)]			Annealed at 250 °C[a)]		
	Mobility [$cm^2 V^{-1} s^{-1}$]	V_{th} [V]	I_{on}/I_{off}	Mobility [$cm^2 V^{-1} s^{-1}$]	V_{th} [V]	I_{on}/I_{off}	Mobility [$cm^2 V^{-1} s^{-1}$]	V_{th} [V]	I_{on}/I_{off}
p-channel	0.064	–11	10^7	0.062	–11	10^7	0.063	–11	10^7
n-channel	0.079	12	10^7	0.078	12	10^7	0.077	12	10^7

[a)]OFETs were thermally annealed on a temperature-controlled hot plate for 15 min under ambient conditions.

that electron-withdrawing trifluoromethyl groups successfully introduce n-channel characteristics into thienylenevinylene-containing conjugated polymers which are generally classified as p-type semiconductors. Furthermore, the smooth and non-s-shaped curves at linear regimes for both p- and n-channel in the output characteristics of CF_3-PBTV based OFET, as shown in Figure 3a, imply the relatively low contact resistance at the interface. The well-equivalent hole and electron mobilities with nearly symmetrical output and transfer characteristics indicate the unique combination of the electron-donating thienylenevinylene as the donor and electron-withdrawing trifluoromethyl-substituted phenyl as the acceptor. Even though DPP-based conjugated copolymers have been reported to have high ambipolar mobilities recently, conjugated copolymers based on our concise molecule design can also provide an alternative to reach ambipolarity.

The threshold voltage (V_{th}) and on/off ratio (I_{on}/I_{off}) were estimated to be –11 V and 10^7 for p-channel, and 12 V and 10^7 for n-channel, as shown in Figure 3b and Table 3. Compared to the on/off ratio (10^2–10^5) of ambipolar OFETs based on low-bandgap (0.96–1.87 eV) conjugated polymers, the on/off ratio (10^7) of ambipolar CF_3-PBTV based OFET is around 2–5 orders higher.[9a,44] The high on/off ratio might be resulted from the relatively large bandgap of CF_3-PBTV which prevents the leakage of off current. The low-lying HOMO energy level of CF_3-PBTV also contributed to the high on/off ratio by precluding the oxygen doping which was reported to increase the off current.[45]

Finally, the long-term stability of CF_3-PBTV based OFET was investigated under ambient conditions. The OFET performance remained almost identical after 90 days in ambient conditions, as summarized in Figure 3c and Table 3. The charge mobilities were slightly decreased from 0.065 and 0.078 $cm^2 V^{-1} s^{-1}$ to 0.062 and 0.071 $cm^2 V^{-1} s^{-1}$ for p- and n-channel, respectively. The extremely high ambient-stability of CF_3-PBTV might be due to its low-lying HOMO energy level (–5.30 eV) resulted from the introduction of strong electron-withdrawing trifluoromethyl groups. In addition, the enhanced resistance to the diffusion of moisture from the hydrophobicity of fluorine atoms might also contribute to the enhanced ambient-stability.

It is generally believed that the thermal annealing process has a profound effect on OFET characteristics. For example, the OFET mobilities were found to be improved from 5.0×10^{-4} to 3.7×10^{-3} $cm^2 V^{-1} s^{-1}$ for p-channel, and from 7.9×10^{-5} to 5.8×10^{-4} $cm^2 V^{-1} s^{-1}$ for n-channel based on a benzodipyrrolidone-based conjugated polymer after thermal annealing at 250 °C for 10 min.[44c] The similar enhancement on the charge mobility of a naphthalene-based conjugated polymer after thermal annealing was also reported.[44a] Therefore, in order to further investigate the optical and OFET characteristics of CF_3-PBTV, thin films and devices were thermally annealed at different temperatures (120, 180, and 250 °C) on a temperature-controlled hot plate under ambient conditions for 15 min. Surprisingly, the maximum absorption of a spin-coated CF_3-PBTV thin film on quartz substrate remained nearly identical at wavelength λ_{max} = 421–422 nm with a vibronic absorption shoulder at wavelength λ_s = 437–438 nm, as shown in Figure S12, Supporting Information. Moreover, the performance of CF_3-PBTV based OFET was independent of the annealing temperatures, as shown in **Table 4**. The charge mobilities were slightly decreased from 0.065 and 0.078 $cm^2 V^{-1} s^{-1}$ to 0.063 and 0.077 $cm^2 V^{-1} s^{-1}$ for p- and n-channel, respectively, after thermal-annealing at 250 °C for 15 min. Moreover, the threshold voltage and on/off ratio remained unchanged after thermal-annealing. The main reason for its annealing-independent property and the structural difference after annealing are still under investigation. However, the annealing-free characteristic of CF_3-PBTV is beneficial to simplify the device fabrication processes.

3. Conclusion

We have successfully synthesized a novel conjugated polymer CF_3-PBTV consisting of thienylenevinylene as the donor and CF_3-BP as the acceptor. CF_3-PBTV shows solution-processability without electrically insulating long alkyl side chains. GI-XRD results suggest a nearly equal population of flat-on and end-on orientated CF_3-PBTV domains in the thin film. The ambipolarity of CF_3-PBTV is demonstrated by well-equivalent charge mobilities of 0.065 and 0.078 $cm^2 V^{-1} s^{-1}$ for p- and n-channel, respectively. Unlike OFETs based on low bandgap conjugated polymers, CF_3-PBTV based OFET shows very high on/off ratio (higher than 10^7) which might be resulted from the relatively large bandgap and low-lying HOMO of CF_3-PBTV. CF_3-PBTV based OFET also demonstrates excellent ambient-stability. The OFET performance barely changed after the device is stored in ambient conditions for 90 days. The ambient-stability of CF_3-PBTV could be attributed to the enhanced oxidative stability from its low-lying HOMO energy level and the better moisture resistance from its fluorine contents. Furthermore, the performance of CF_3-PBTV-based OFET is annealing independent. It is noteworthy that the solution-processable, ambipolar, and thienylenevinylene-containing conjugated polymer without any long alkyl side chains is reported for the first time. And to the best of our knowledge, it is the first ambient-stable, annealing-free OFET with well-equivalent ambipolarity.

4. Experimental Section

General: Monomers (2)–(8) were synthesized according to the procedures in our previous publications as shown in Scheme S1, Supporting Information.[46] Tetrabutylammonium perchlorate (TBAP) used in cyclic voltammetric measurements was recrystallized twice with ethyl acetate and dried at 120 °C under reduced pressure overnight. All of other reagents were purchased from commercial companies and used as received. All of the solvents used in this communication were purified according to standard method prior to use. All melting points were determined on a Mel-Temp capillary melting point apparatus. ^{1}H NMR and ^{13}C NMR spectra were measured at 500 and 125 MHz on a Bruker Avance-500 spectrometer, respectively. Mass spectroscopy was conducted on a Finnigan TSQ 700 mass spectrometer. Elemental analyses were performed on Heraeus Vario analyzer. Molecular weights were measured on a JASCO GPC system (PU-980) equipped with an RI detector (RI-930), a Jordi Gel DVB Mixed Bed column (250 × 10 mm) column, using N,N-dimethylacetamide (DMAc) as the eluent and calibrated with polystyrene standards. Thermogravimetric analysis (TGA) was performed in nitrogen with a TA TGA Q500 thermogravimetric analyzer using a heating rate of 10 °C min^{-1}. Differential scanning calorimetry (DSC) measurements were carried out under N_2 atmosphere using a PerkineElmer DSC 4000 analyzer at a heating rate of 10 °C min^{-1}. UV–vis spectrometry was carried out on a JASCO V-670 UV–vis/NIR spectrophotometer. Cyclic voltammetric (CV) measurements were carried out on a CH Instrument 611C electrochemical analyzer at room temperature in a three-electrode electrochemical cell with a working electrode (polymer film coated on ITO glass), a reference electrode (Ag/Ag$^+$, referenced against ferrocene/ferrocenium (Fc/Fc$^+$), 0.09 V), and a counter electrode (Pt gauze) at a scan rate of 100 mV s^{-1}. CV measurements for polymer films were performed in an electrolyte solution of 0.1 M tetrabutylammonium perchlorate (TBAP) in acetonitrile. The potential window at oxidative scan and reductive scan was 0–2.0 V and 0 to −2.0 V, respectively. Grazing-incidence X-ray diffraction measurement (GI-XRD) was performed on a Bruker AXS GmbH/NANOSTAR U diffractometer using a Typhoon FLA 7000 image plate detector with the wavelength of $\lambda = 1.541$ Å. The samples were prepared following the same procedures for OFET devices without gold electrodes.

Synthesis of 2,2′-Bis(trifluoromethyl)-4,4′-bis(diethyl methylenephosphonate)-biphenyl (9): To a 100 mL, three-necked, round bottomed flask were added 2,2′-bis(trifluoromethyl)-4,4′-bis(bromomethyl)biphenyl (8)[46] (0.67 g, 1.41 mmol) and triethyl phosphate (0.72 mL, 4.22 mmol). The reaction mixture was stirred and heated to reflux for 24 h. The excess triethyl phosphate was removed by distillation at 120 °C to afford brown oil-like crude product. The crude product was further purified by column chromatography using ethyl acetate as eluent to afford 0.56 g of pale yellow oil-like product (68%): ^{1}H NMR (500 MHz, DMSO-d_6, δ, ppm): 7.75 (s, 2H; Ar-H$_a$), 7.60 (d, J = 7.9 Hz, 2H; Ar-H$_c$), 7.32 (d, J = 7.9 Hz, 2H; Ar-H$_b$), 3.98 (m, J = 7.1 Hz, 8H; H$_e$), 3.43 (d, J = 21.7 Hz, 4H; H$_d$), 1.16 (m, J_1 = 7.1 Hz, J_2 = 2.4 Hz, 12H; H$_f$) as shown in Figure S1, Supporting Information; ^{13}C NMR (125 MHz, DMSO-d_6, δ, ppm): 127.69, 127.45, 127.19, 126.98 (q, C$_6$), 127.17, 124.98, 122.80, 120.62 (q, C$_7$), 134.87 (C$_1$), 133.69 (C$_5$), 132.87 (C$_3$), 131.61 (C$_2$), 129.49 (C$_4$), 61.69 (C$_8$), 31.73 (C$_9$), 16.06 (C$_{10}$) as shown in Figure S2, Supporting Information; EIMS (m/z): Calcd. for $C_{24}H_{30}F_6O_6P_2$: 590.1; Found: 590.3 [M]$^+$. Anal. Calcd for $C_{24}H_{30}F_6O_6P_2$: C 48.82, H 5.12; found: C 48.92, H 5.32.

Synthesis of CF$_3$-PBTV: To a 100 mL, three-neck, round-bottom flask were added 2,2′-bis(trifluoromethyl)-4,4′-bis(diethyl methylenephosphonate)biphenyl (9) (0.31 g, 0.52 mmol), thiophene-2,5-dicarbaldehyde (0.07 g, 0.52 mmol), and anhydrous DMF (12.6 mL). 1.0 M *t*-BuOK (4.14 mL, 2.10 mmol, in THF solution) was slowly added with a syringe under nitrogen atmosphere. The reaction mixture was further stirred at room temperature for 48 h under nitrogen atmosphere. The reaction mixture was then poured into water. The precipitate that formed was collected by filtration and washed with hot methanol (Soxhlet apparatus) for 24 h and dried at 100 °C overnight under reduced pressure to afford 0.20 g of brown solids (yield: 91%). ^{1}H NMR (500 MHz, DMSO-d_6, δ, ppm): 8.08 (s, 2H; Ar-H$_e$), 7.93 (s, 2H; Ar-H$_d$), 7.74 (d, J = 15 Hz, 1H; C = C-H$_c$), 7.39 (s, 2H; H$_f$), 7.29 (s, 2H; H$_a$), 7.15 (d, J = 15 Hz, 1H; C = C-H$_b$) as shown in Figure S3, Supporting Information; ^{13}C NMR (125 MHz, DMSO-d_6, δ, ppm): 130.02, 129.74, 129.46, 129.16 (q, C$_9$), 127.09, 125.03, 123.01, 120.94 (q, C$_{11}$), 135.15 (C$_5$), 133.00 (C$_{10}$), 130.97 (C$_6$), 128.20 (C$_8$), 127.81 (C$_7$), 127.37 (C$_4$), 126.46 (C$_3$), 124.16 (C$_1$), 122.58 (C$_2$) as shown in Figure S4, Supporting Information; Anal. Calcd for $C_{22}H_{14}F_6S$: C 62.55, H 2.87; found: C 61.99, H 2.65.

Synthesis of PBPV: To a 100 mL, three-neck, round-bottom flask were added 2,2′-bis(trifluoromethyl)-4,4′-bis(diethyl methylenephosphonate) biphenyl (9) (0.53 g, 0.90 mmol), 2,2′-bis(trifluoromethyl)-4,4′-biphenyldicarbaldehyde (6) (0.31 g, 0.90 mmol), and anhydrous DMF (42.0 mL). 1.0 M *t*-BuOK (7.00 mL, 7.00 mmol, in THF solution) was slowly added with a syringe under nitrogen atmosphere. The reaction mixture was further stirred at room temperature for 48 h under nitrogen atmosphere. The reaction mixture was then poured into water. The precipitate that formed was collected by filtration and washed with hot methanol (Soxhlet apparatus) for 24 h and dried at 100 °C overnight under reduced pressure to afford 0.45 g of yellow solids (yield: 80%). ^{1}H NMR (500 MHz, DMF-d_7, δ, ppm): 8.28 (s, 2H; Ar-H$_d$), 8.14 (s, 2H; Ar-H$_c$), 7.78 (s, 2H; Ar-H$_b$), 7.58 (s, 2H; H$_a$) as shown in Figure S8, Supporting Information; ^{13}C NMR (125 MHz, DMF-d_7, δ, ppm): 130.22, 129.94, 129.66, 129.38 (q, C$_6$), 127.41, 125.31, 123.21, 121.11 (q, C$_8$), 134.14 (C$_2$), 132.12 (C$_7$), 131.01 (C$_3$), 128.93 (C$_5$), 128.11 (C$_4$), 127.92 (C$_1$) as shown in Figure S9, Supporting Information; Anal. Calcd for $C_{16}H_8F_6$: C 61.14, H 2.57; found: C 60.70, H 2.39. M_n: 15 000 g mol^{-1}; M_w: 29 000 g mol^{-1}; PDI: 1.93; T$_d$: 417 °C; Char yield: 53%.

Organic Field-Effect Transistor Fabrication and Characterization: All fabrication processes, except SiO$_2$ growth and gold evaporation, were performed in ambient conditions in a conventional hood. OFET devices were fabricated with a bottom-gate, top-contact configuration. Thin polymeric semiconductor films were deposited by spin-coasting at 1000 rpm for 30 s of a 5 mg mL^{-1} CF$_3$-PBTV solution in anhydrous DMF onto *n*-octadecyltrichlorosilane (OTS)-modified heavily doped n^+-Si wafer with thermally grown SiO$_2$ dielectric layer (200 nm). The capacitance of SiO$_2$ gate insulator was 11 nF cm^{-2}. Prior to the treatment of OTS, the wafers were sonication-cleaned by acetone and isopropanol, sequentially, and were then dried at 100 °C for 10 min in vacuum oven. The drain and source electrode were obtained by thermally evaporated gold (Au, 30 nm) through a shadow mask. The channel width (W) and length (L) were 2000 and 50 μm, respectively. All the OFET characteristics were measured with a Keithley 4200-SCS semiconductor characterization system at room temperature in ambient conditions. Key device parameters, such as charge mobilities (μ) and on/off ratio (I_{on}/I_{off}) were obtained from the source-drain current (I_{DS}) versus gate-source voltage (V_{GS}) characteristics employing standard procedures. Mobilities were extracted from the formula defined by saturation regime in transfer plots, $\mu = 2I_{DS}L\ [C_iW(V_{GS} - V_{th})^2]^{-1}$, where V_{th} is the threshold voltage. Threshold voltage was obtained from the intercept of V_{GS} versus $I_{DS}^{1/2}$ plots. OFETs were stored under ambient conditions for 90 days in a conventional hood for the long-term ambient-stability measurement. OFETs were thermally annealed on a temperature-controlled hot plate under ambient conditions in a conventional hood for the annealing-temperature-independent measurement.

DFT Simulation: Density functional theory (DFT) calculations were performed using the B3LYP functional[35] and the 6–31 G** basis set[36] as implemented in GAUSSIAN 09.

Supporting Information

Supporting Information is available from the Wiley Online Library or from the author.

Received: October 1, 2014
Revised: November 14, 2014
Published online:

[1] a) U. Zschieschang, T. Yamamoto, K. Takimiya, H. Kuwabara, M. Ikeda, T. Sekitani, T. Someya, H. Klauk, *Adv. Mater.* **2011**, *23*, 654; b) B. Kang, W. H. Lee, K. Cho, *ACS Appl. Mater. Interfaces* **2013**, *5*, 2302; c) L. Torsi, M. Magliulo, K. Manoli, G. Palazzo, *Chem. Soc. Rev.* **2013**, *42*, 8612.

[2] a) S. Wang, M. Kappl, I. Liebewirth, M. Müller, K. Kirchhoff, W. Pisula, K. Müllen, *Adv. Mater.* **2012**, *24*, 417; b) C. Wang, H. Dong, W. Hu, Y. Liu, D. Zhu, *Chem. Rev.* **2012**, *112*, 2208.

[3] a) H. Yan, Z. Chen, Y. Zheng, C. Newman, J. R. Quinn, F. Dötz, M. Kastler, A. Facchetti, *Nature* **2009**, *457*, 679; b) Y. Li, S. P. Singh, P. Sonar, *Adv. Mater.* **2010**, *22*, 4862.

[4] a) S. Holliday, J. E. Donaghey, I. McCulloch, *Chem. Mater.* **2014**, *26*, 647; b) C. B. Nielsen, I. McCulloch, *Prog. Polym. Sci.* **2013**, *38*, 2053.

[5] a) W. S. Yoon, S. K. Park, I. Cho, J. A. Oh, J. H. Kim, S. Y. Park, *Adv. Funct. Mater.* **2013**, *23*, 3519; b) J. C. Bijleveld, A. P. Zoombelt, S. G. J. Mathijssen, M. M. Wienk, M. Turbiez, D. M. de Leeuw, R. A. Janssen, *J. Am. Chem. Soc.* **2009**, *131*, 16616; c) C. B. Nielsen, M. Turbiez, I. McCulloch, *Adv. Mater.* **2013**, *25*, 1859; d) C. Kanimozhi, N. Yaacobi-Gross, K. W. Chou, A. Amassian, T. D. Anthopoulos, S. Patil, *J. Am. Chem. Soc.* **2012**, *134*, 16532; e) B. Sun, W. Hong, Z. Yan, H. Aziz, Y. Li, *Adv. Mater.* **2014**, *26*, 2636; f) H. J. Yun, S. J. Kang, Y. Xu, S. O. Kim, Y. H. Kim, Y. Y. Noh, S. K. Kwon, *Adv. Mater.* **2014**, *26*, 7300.

[6] a) J. D. Yuen, R. Kumar, D. Zakhidov, J. Seifter, B. Lim, A. J. Heeger, F. Wudl, *Adv. Mater.* **2011**, *23*, 3780; b) J. Fan, J. D. Yuen, M. Wang, J. Seifter, J. H. Seo, A. R. Mohebbi, D. Zakhidov, A. Heeger, F. Wudl, *Adv. Mater.* **2012**, *24*, 2186.

[7] a) J. C. Chen, H. C. Wu, C. J. Chiang, L. C. Peng, T. Chen, L. Xing, S. W. Liu, *Polymer* **2011**, *52*, 6011; b) J. C. Chen, H. C. Wu, C. J. Chiang, T. Chen, L. Xing, *J. Mater. Chem. C* **2014**, *2*, 4835.

[8] a) T. Lei, J. Y. Wang, J. Pei, *Acc. Chem. Res.* **2014**, *47*, 1117; b) T. Lei, J. H. Dou, Z. J. Ma, C. H. Yao, C. J. Liu, J. Y. Wang, J. Pei, *J. Am. Chem. Soc.* **2012**, *134*, 20025; c) P. Deng, Q. Zhang, *Polym. Chem.* **2014**, *5*, 3298.

[9] a) K. C. Lee, W. T. Park, Y. Y. Noh, C. Yang, *ACS Appl. Mater. Interfaces* **2014**, *6*, 4872; b) J. W. Rumer, M. Levick, S. Y. Dai, S. Rossbauer, Z. Huang, L. Biniek, T. D. Anthopoulos, J. R. Durrant, D. J. Procter, I. McCulloch, *Chem. Commun.* **2013**, *49*, 4465; c) G. W. P. van Pruissen, E. A. Pidko, M. M. Wienk, R. A. J. Janssen, *J. Mater. Chem. C* **2014**, *2*, 731; d) W. Cui, J. Yuen, F. Wudl, *Macromolecules* **2011**, *44*, 7869.

[10] a) M. Sommer, *J. Mater. Chem. C* **2014**, *2*, 3088; b) J. E. Anthony, A. Facchetti, M. Heeney, S. R. Marder, X. Zhan, *Adv. Mater.* **2010**, *22*, 3876; c) X. Zhan, A. Facchetti, S. Barlow, T. J. Marks, M. A. Ratner, M. R. Wasielewski, S. R. Marder, *Adv. Mater.* **2011**, *23*, 268.

[11] J. E. Anthony, *Chem. Mater.* **2011**, *23*, 583.

[12] M. L. Tang, Z. Bao, *Chem. Mater.* **2011**, *23*, 446.

[13] a) Z. Chen, M. J. Lee, R. S. Ashraf, Y. Gu, S. Albert-Seifried, M. M. Nielsen, B. Schroeder, T. D. Anthopoulos, M. Heeney, I. McCulloch, *Adv. Mater.* **2012**, *24*, 647; b) J. D. Yuen, J. Fan, J. Seifter, B. Lim, R. Hufschmid, A. J. Heeger, F. Wudl, *J. Am. Chem. Soc.* **2011**, *133*, 20799; c) J. Lee, A.-R. Han, J. Kim, Y. Kim, J. H. Oh, C. Yang, *J. Am. Chem. Soc.* **2012**, *134*, 20713; d) J. Lee, A.-R. Han, H. Yu, T. J. Shin, C. Yang, J. H. Oh, *J. Am. Chem. Soc.* **2013**, *135*, 9540; e) J. Li, Y. Zhao, H. S. Tan, Y. Guo, C. A. Di, G. Yu, Y. Liu, M. Lin, S. H. Lim, Y. Zhou, H. Su, B. S. Ong, *Sci. Rep.* **2012**, *2*, 754.

[14] J. L. Brédas, A. J. Heeger, *Chem. Phys. Lett.* **1994**, *217*, 507.

[15] E. J. Meijer, D. M. de Leeuw, S. Setayesh, E. van Veenendaal, B. H. Huisman, P. W. M. Blom, J. C. Hummelen, U. Scherf, T. M. Klapwijk, *Nat. Mater.* **2003**, *2*, 678.

[16] B. Lim, K. J. Baeg, H. G. Jeong, J. Jo, H. Kim, J. W. Park, Y. Y. Noh, D. Vak, J. H. Park, J. W. Park, D. Y. Kim, *Adv. Mater.* **2009**, *21*, 2808.

[17] a) H. E. Katz, A. J. Lovinger, J. Johnson, C. Kloc, T. Siegrist, W. Li, Y. Y. Lin, A. Dodabalapur, *Nature* **2000**, *404*, 478; b) T. Huang, X. Wang, T. Malmgren, K. Hong, J. W. Mays, *Macromol. Chem. Phys.* **2012**, *213*, 49.

[18] a) L. Li, D. M. Collard, *Macromolecules* **2006**, *39*, 6092; b) N. Terasawa, H. Monobe, K. Kiyohara, *J. Fluorine Chem.* **2006**, *127*, 954.

[19] a) K. Reichenbächer, H. I. Süss, J. Hulliger, *Chem. Soc. Rev.* **2005**, *34*, 22; b) Y. Wang, S. R. Parkin, J. Gierschner, M. D. Watson, *Org. Lett.* **2008**, *10*, 3307.

[20] A. Babel, S. A. Jenekhe, *J. Am. Chem. Soc.* **2003**, *125*, 13656.

[21] G. Yu, J. Gao, J. C. Hummelen, F. Wudl, A. J. Heeger, *Science*, **1995**, *270*, 1789.

[22] J. C. Bijleveld, V. S. Gevaerts, D. D. Nuzzo, M. Turbiez, S. G. J. Mathijssen, D. M. de Leeuw, M. M. Wienk, R. A. J. Janssen, *Adv. Mater.* **2010**, *22*, E242.

[23] J. K. J. van Duren, X. Yang, J. Loos, C. W. T. Bulle-Lieuwma, A. B. Sieval, J. C. Hummelen, R. A. J. Janssen, *Adv. Funct. Mater.* **2004**, *14*, 425.

[24] a) J. Mei, D. H. Kim, A. L. Ayzner, M. F. Toney, Z. Bao, *J. Am. Chem. Soc.* **2011**, *133*, 20130; b) J. Mei, Z. Bao, *Chem. Mater.* **2014**, *26*, 604.

[25] a) A. Y. Amin, A. Khassanov, K. Reuter, T. Meyer-Friedrichsen, M. Halik, *J. Am. Chem. Soc.* **2012**, *134*, 16548; b) H. Meng, J. Zheng, A. J. Lovinger, B. C. Wang, P. G. V. Patten, Z. Bao, *Chem. Mater.* **2003**, *15*, 1778.

[26] M. Halik, H. Klauk, U. Zschieschang, G. Schmid, S. Ponomarenko, S. Kirchmeyer, W. Weber, *Adv. Mater.* **2003**, *15*, 917.

[27] a) J. Rivnay, M. F. Toney, Y. Zheng, I. V. Kauvar, Z. Chen, V. Wagner, A. Facchetti, A. Salleo, *Adv. Mater.* **2010**, *22*, 4359; b) S. Fabiano, C. Musumeci, Z. Chen, A. Scandurra, H. Wang, Y. L. Loo, A. Facchetti, B. Pignataro, *Adv. Mater.* **2012**, *24*, 951.

[28] a) A. Facchetti, M. H. Yoon, C. L. Stern, G. R. Hutchison, M. A. Ratner, T. J. Marks, *J. Am. Chem. Soc.* **2004**, *126*, 13480; b) K. Geramita, Y. Tao, R. A. Segalman, T. D. Tilley, *J. Org. Chem.* **2010**, *75*, 1871.

[29] a) F. Babudri, G. M. Farinola, F. Naso, R. Ragni, *Chem. Commun.* **2007**, *10*, 1003; b) Y. Geng, K. Tajima, K. Hashimoto, *Macromol. Rapid Commun.* **2011**, *32*, 1478.

[30] A. Fleissner, K. Stegmaier, C. Melzer, H. von Seggern, T. Schwalm, M. Rehahn, *Chem. Mater.* **2009**, *21*, 4288.

[31] U. H. F. Bunz, *Chem. Rev.* **2000**, *100*, 1605.

[32] a) F. Qing, Y. Sun, X. Wang, N. Li, Y. Li, X. Li, H. Wang, *Polym. Chem.* **2011**, *2*, 2102; b) C. Zhang, T. Matos, R. Li, S. S. Sun, J. E. Lewis, J. Zhang, X. Jiang, *Polym. Chem.* **2010**, *1*, 663; c) B. Lim, J. S. Yeo, D. Khim, D. Y. Kim, *Macromol. Rapid Commun.* **2011**, *32*, 1551.

[33] a) J. C. Chen, Y. C. Liu, J. J. Ju, C. J. Chiang, Y. T. Chern, *Polymer* **2011**, *52*, 954; b) J. C. Chen, C. J. Chiang, Y. C. Liu, *Synth. Met.* **2010**, *160*, 1953.

[34] W. Zhang, J. Smith, S. E. Watkins, R. Gysel, M. McGehee, A. Salleo, J. Kirkpatrick, S. Ashraf, T. Anthopoulos, M. Heeney, I. McCulloch, *J. Am. Chem. Soc.* **2010**, *132*, 11437.

[35] A. D. Becke, *J. Chem. Phys.* **1993**, *98*, 1372.

[36] M. M. Franci, W. J. Pietro, W. J. Hehre, J. S. Binkley, M. S. Gordon, D. J. DeFrees, J. A. Pople, *J. Chem. Phys.* **1982**, *77*, 3654.

[37] V. Senkovskyy, R. Tkachov, T. Beryozkina, H. Komber, U. Oertel, M. Horecha, V. Bocharova, M. Stamm, S. A. Gevorgyan, F. Krebs, A. Kirity, *J. Am. Chem. Soc.* **2009**, *131*, 16445.

[38] K. M. Coakley, B. S. Srinivasan, J. M. Ziebarth, C. Goh, Y. Liu, M. D. McGehee, *Adv. Funct. Mater.* **2005**, *15*, 1927.

[39] G. Lu, L. Li, X. Yang, *Adv. Mater.* **2007**, *19*, 3594.

[40] M. Aryal, K. Trivedi, W. Hu, *ACS Nano* **2009**, *3*, 3085.

[41] J. Ma, K. Hashimoto, T. Koganezawa, K. Tajima, *J. Am. Chem. Soc.* **2013**, *135*, 9644.
[42] X. M. Hong, J. C. Tyson, D. M. Collard, *Macromolecules* **2000**, *33*, 3502.
[43] H. Sirringhaus, P. J. Brown, R. H. Friend, M. M. Nielsen, K. Bechgaard, B. M. W. Langeveld-Voss, A. J. H. Spiering, R. A. J. Janssen, E. W. Meijer, P. Herwig, D. M. de Leeuw, *Nature* **1999**, *401*, 685.
[44] a) F. S. Kim, X. Guo, M. D. Watson, S. A. Jenekhe, *Adv. Mater.* **2010**, *22*, 478; b) T. T. Steckler, P. Henriksson, S. Mollinger, A. Lundin, A. Salleo, M. R. Andersson, *J. Am. Chem. Soc.* **2014**, *136*, 1190; c) N. B. Kolhe, A. Z. Ashar, K. S. Narayan, S. K. Asha, *Macromolecules* **2014**, *47*, 2296.
[45] I. Osaka, R. Zhang, G. Sauvé, D. M. Smilgies, T. Kowalewski, R. D. McCullough, *J. Am. Chem. Soc.* **2009**, *131*, 2521.
[46] J. C. Chen, C. J. Chiang, J. C. Chiu, J. J. Ju, *Chem. Commun.* **2012**, *48*, 7756.